Journal of Ceramic Processing Research. Vol. 21, No. 2, pp. 256~262 (2020)
(Received 15 January 2020, Received in revised form 19 March 2020, Accepted 20 March 2020)
https://doi.org/10.36410/jcpr.2020.21.2.256

J O U R N A L O F
Ceramic Processing Research

Investigation of the electrical properties of Ag/n-Si schottky diode obtained by two different methods

Vagif Nevruzoglu*, Melih Manir and Gizem Ozturk
Department of Energy Systems Engineering, Recep Tayyip Erdogan University, 53100 Rize, Turkey

In present study, Ag/n-Si Schottky diodes were produced by vacuum evaporation method at two different substrate temperatures (200 K and 300 K) and structural, optical, electrical properties were investigated. X-ray diffraction studies showed that the textures of the Ag films are cubic with a strong (111) preferred direction. Field emission scanning electron microscopy (FESEM) images revealed that the Ag layer coated at 200 K substrate temperature consisted of nano clusters of equal size (12-15 nm) and the Ag layer consisted of islets of different sizes (80-100 nm) at 300 K substrate temperature. The ideal factor (n), barrier height (φ_B), saturation current (I_0) and series resistance (R_S) for Schottky diodes 200 K and 300 K substrate temperature produced, obtained by using I-V measurements respectively 1.11, 0.85 eV, 0.0014 ηA, 3.45 KΩ and 3.68, 0.78 eV, 0.05 ηA, 5.51 KΩ. Donor density (N_D) and flat band potential (E_{FB}) for Schottky diodes 200 K and 300 K substrate temperature produced, obtained by using C-V measurements respectively 1.1×10^{15} cm^{-3}, 0.52 V and 1.4×10^{16} cm^{-3}, 0.34 V. When the characteristic properties of Schottky diodes are examined, it is understood that the differences depending on the method are caused by the distribution of homogeneous and equal sized nano clusters on the Si surface of the Ag layer produced at 200 K substrate temperature.

Keywords: Cold substrate, Thin film, Schottky diode.

Introduction

Metal-semiconductor contacts (Schottky diodes) are indispensable component of the electronics industry. Compared to P-N junction, these devices have some advantages such as low series resistance, high power capacity and high switching speed at low voltage values [1, 2]. The electrical parameters of an ideal Schottky diode are determined by the properties of the metal-semiconductor interface region [3, 4]. In this direction, metal layers are formed by different methods and an intermediate layer is placed in the metal-semiconductor contact area [5, 6]. Nowadays, Schottky diodes, transistor and solar cells are produced using different methods such as thermal evaporation, spin coater and magnetron sputtering [7-9]. Micro and nano structured materials are becoming increasingly important in technology [10].

Ag/SiO_2/n-Si Schottky diode was produced and examined by with vacuum evaporation technique. The electrical characteristics of the metal-insulator-semiconductor diode and the interface state density were evaluated by I-V and impedance spectroscopy. They calculated the barrier height as 0.62 eV, the ideality factor as 1.91 and the average series resistance as 975.8 Ω [11].

*Corresponding author:
Tel : +90 464 2237518
Fax: +90 464 2237514
E-mail: vagif.nevruzoglu@erdogan.edu.tr

Bates et al. (2007) showed that Ag atoms have deposited on the surface of n-Si at 400 and 550 ºC by using magnetron sputtering technique. They found that Ag grain size at 400 ºC from TEM images was 5 nm and 10 nm at 550 ºC. In Schottky diode produced at 400 ºC, carrier density is smaller than 550 ºC. However, resistance and mobility values of Ag layer produced at 400 ºC were higher than 550 ºC [12]. Mahmood et al. (2018) examined Ag/n-Si diodes by creating some of the characteristics of these diodes with the organic interface layer and non-interface layer. The ideality factor of the structures with non-interface layer and the organic interface layer was 1.42 and 1.83 respectively. The size of the barrier height was 0.65 eV for the Ag/n-Si structure and 0.66 eV for the hybrid structure. The series resistance values of the structures with and without organic interface layer were 7,839 Ω and 135 respectively. Donor density was 2.07×10^{14} cm^{-3} in the Ag / n-Si structure and 24.8×10^{14} cm^{-3} in the hybrid structure [13]. Korosak and Cvikl (1998) used Ionized Cluster Ray (ICB) method and obtained the Ag/n-Si Schottky structures current voltage characteristics measured at different temperature ranges (300 K-150 K). In the examples, different current conduction mechanisms were determined [14].

Clayton et al. (2013) revealed that Ag/n-Si composite films produced by magnetron sputtering technique at 550 ºC on n-Si (111) substrates were characterized. Films were prepared with a concentration of 13, 16 and 22% Ag and measured in the 77-500 K temperature

range. A decrease in resistance values was observed between the Ag nanoparticles formed with increasing Ag concentration due to less grain boundary. It was found that as Ag concentration increased, grain boundaries converged and became ineffective. The barrier heights were found to be 0.360 eV, 0.390 eV and 0.470 eV for the films with Ag concentrations of 13%, 16% and 22%, respectively. As can be seen from the studies mentioned above, the characteristics of Schottky diodes change depending on the production method [15].

In the study conducted by Yüzüak et al. (2019), Ag layers were grown by soliton growth mechanism on n-Si (100) substrates by using cold substrate method [16]. Some characteristics of the diode obtained at 200 K substrate temperature were compared with those of the diode produced at 300 K substrate temperature.

As mentioned above, in literature studies, the studies using cold substrate method exist. However, based on our best knowledge, there is no a study examining the effect of this technique on the characteristics of Ag/n-Si Schottky structures which forms the basis of the study. Present study was realized by making use of this gap. Recent studies have focused on the surface plasmon resonance (SPR) diffusion model that occurs in nano size metallic particle systems [14]. This model shows more effective diffusion of nano sized metallic particles. The advantages and disadvantages of this model will be revealed in this dual structure we have discussed.

Experimental

In the experiments, n-Si substrates (100) with resistivity value of ρ = 1-10 Ω·cm and thickness of d = 375 μm were used. InGa material was used for ohmic contact on n-Si. Ag/Si binary structures were annealed at room conditions for 30 min at 300 °C due to the formation of diode structure. The cold substrate method view of the evaporation apparatus is given in Fig. 1. Substrate temperature was monitored and controlled using thermocouple. When the pressure reached 1.1×10^{-5} Torr, the substrate was cooled using liquid nitrogen. The Ag thin films were grown at substrate temperatures of 300 K and 200 K. The shutter is continuously kept open during deposition. The Ag thin films were deposited by vacuum evaporation in a quasi-closed volume on n-Si substrates using high purity Ag wire (99.99%) as the source material [16].

The crystal structure of Ag thin films was studied by X-ray diffraction (XRD) using Rigaku SmartLab diffractometer with CuKα radiation (λ = 1,5408 Å) over the range $20^o \leq 2\theta \leq 80^o$ at room temperature. Electrical measurements of n-Si/Ag Schottky diodes were performed at room temperature (300K) using the Ivium CompactStat.h10800 electrochemical measuring device. Zeiss Sigma 300 was used for Field Emission Scanning Electron Microscopy (FESEM) analysis. Changes in the Photocurrent values versus wavelength were studied at room temperature in the range of 350-750 nm by Monora 200 monochramator for Ag layers produced at 200 K and 300 K substrate temperatures.

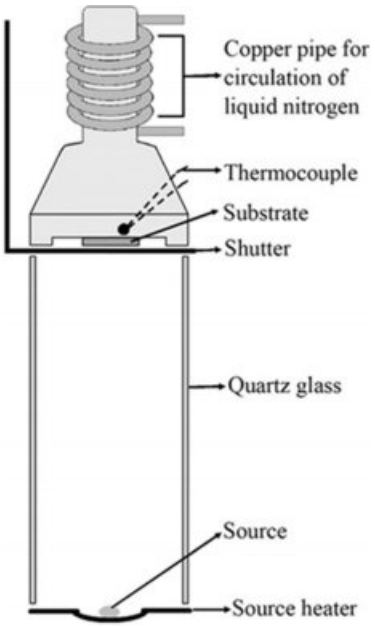

Fig. 1. A cross-sectional view of the thermal evaporation apparatus.

Results and Discussion

The XRD results of the Ag films on n-Si substrates at temperatures of 300 K and 200 K are shown in Fig. 2. X-ray was sent to the substrate surface at angle of 1° and reflected from the Ag thin film. It was found from the XRD patterns that the reflection intensity of the substrate evaporated in Ag layer at 200 K temperature was higher than substrate evaporated at 300 K. This phenomenon is due to forming a tight package on the n-Si surface for the Ag coated substrate at temperature of 200 K. The peaks of Ag layers at angles $2\theta = 38.2^o$, 44.3^o, 64.5^o and 77.6^o belonged to (111), (200), (220) and (311) planes respectively. In addition, it was seen that the Ag thin film was in line with the preferred growth orientation (111) and had a cubic structure [17]. The peaks seen in the XRD pattern were compared with the PDF Card No: 1100136 data card. However, in the spectrum $2\theta = 55^o$, Si (100) plane reflection was detected.

Fig. 3 shows the FESEM image of Ag thin films produced on a glass surface for substrate temperature at 200 K and 300 K. In Fig. 3(a), at 300 K production temperature, Ag layer is composed of islets of different sizes and in Fig. 3(b), at 200 K production temperature, Ag layer is composed of equal sized clusters [18]. This result shows that the Ag layer at substrate temperature of 200 K is caused by soliton growth mechanism.

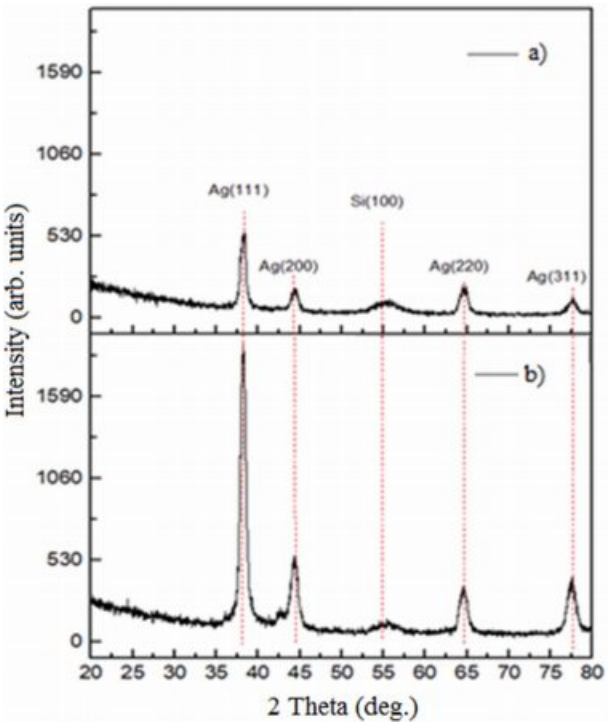

Fig. 2. XRD patterns of n-Si/Ag prepared binary structure at (a) 300 K and (b) 200 K.

As it is known, superficial plasmon resonance (SPR) event occurs in nano-sized Ag layers at a certain frequency [19]. In order to determine this, the changes in the photocurrent values according to the wavelength of Ag layers formed on the insulating glass surface at 300 K and 200 K substrate temperatures were examined. Fig. 4 shows the photocurrent value of the Ag film produced at a substrate temperature of 200 K at a wavelength of 470 nm [19]. The wavelength at which the SPR event occurs corresponds to 638 THz. It is known from the literature that the SPR event in the Ag structure has a frequency of 638 THz [14]. At 300 K substrate temperature, there is no interesting situation in the photocurrent values with varying wavelengths.

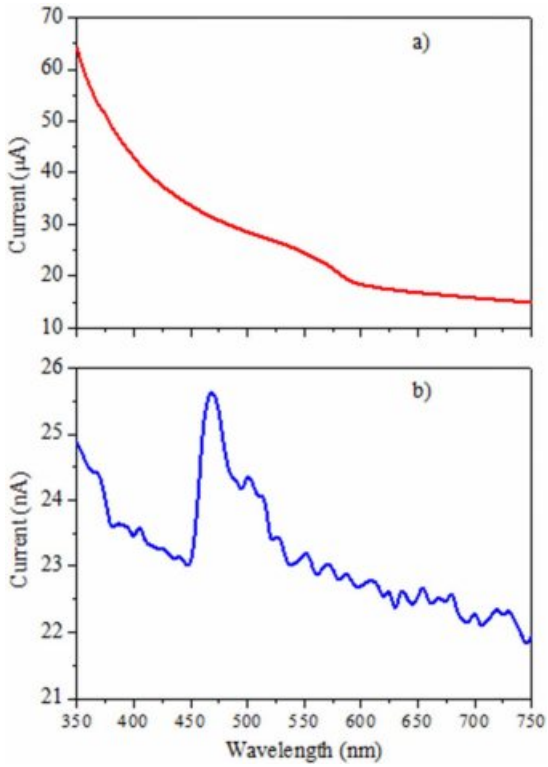

Fig. 4. Wavelength-current graph at (a) 300 K and (b) 200 K.

Fig. 5 shows the I - V measurement results of n-Si/Ag Schottky diodes produced at substrate temperature of 200 K and 300 K. As can be seen, both examples show rectifier characteristics. The n-Si/Ag Schottky diode produced at a substrate temperature of 200 K showed sharper rectifier properties. This was due to reduction in surface state density in the metal-semiconductor contact region of the diode produced at a substrate temperature of 200 K.

The thermionic emission current-voltage relation of a Schottky diode is given by [20]

$$I = I_o e^{qv}/nkT - 1 \quad (1)$$

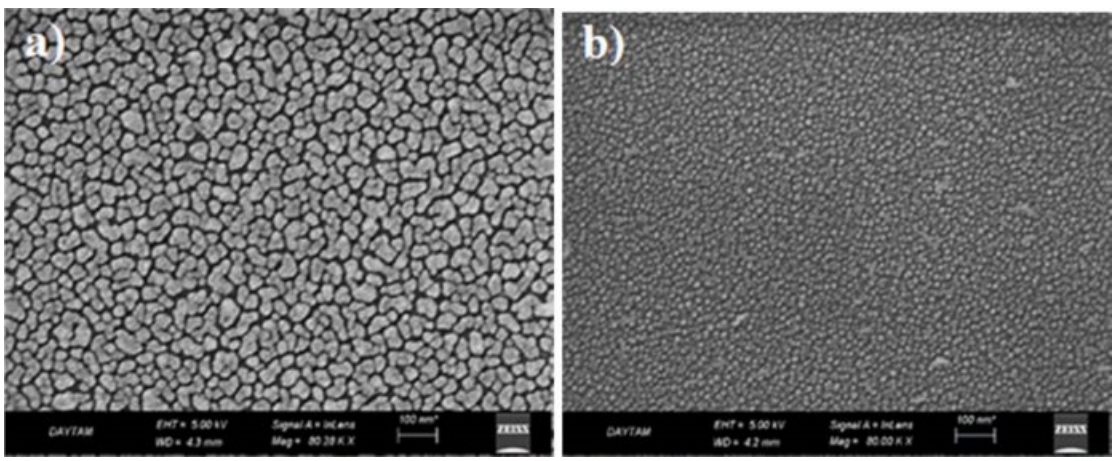

Fig. 3. FESEM image of glass/Ag thin films (a) 300 K and (b) 200 K.

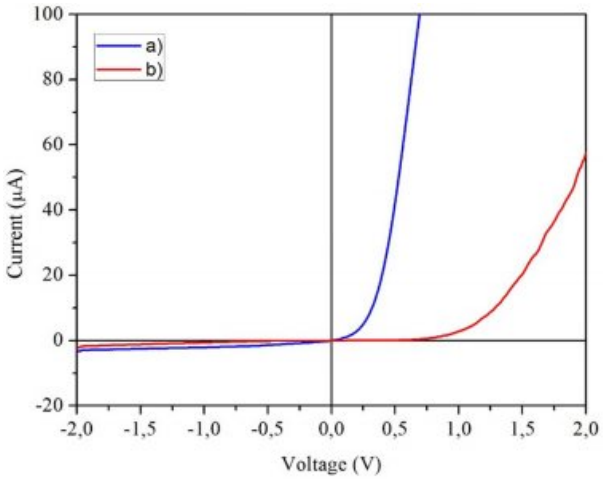

Fig. 5. I-V graph of n-Si/Ag Schottky barriers at (a) 200 K and (b) 300 K.

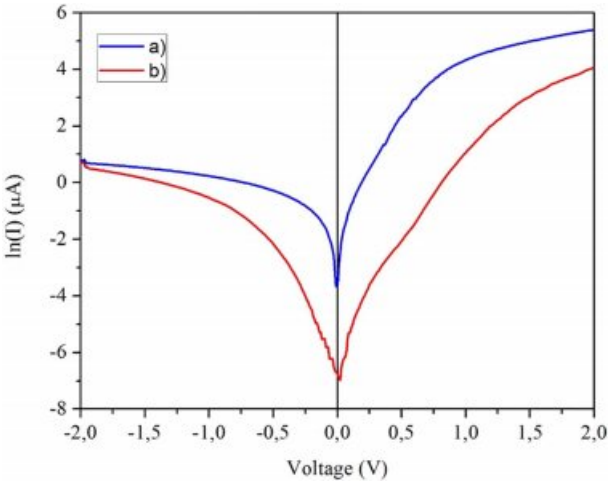

Fig. 6. Semi-logarithmic I-V graph of n-Si/Ag Schottky diode at (a) 200 K and (b) at 300 K.

where I_0 is the saturation current, q is the electronic charge, V is the applied voltage, n is the ideality factor, k is Boltzmann's constant and T is the temperature in K. The saturation current I_0 is defined by

$$I_o = AA^*T^2 e^{\phi_b/kT} \tag{2}$$

where A^* is the theoretical Richardson constant (A^* = 112 A/cm^{2}K^2 for n-Si), A is the diode area and ϕ_b is the zero bias barrier height. For V values greater than 3 kT/q, the ideality factor n can be calculated from the slope of the rectification line region of the forward bias ln(I)-V plot for each temperature and can be written as

$$n = \frac{q}{kT}\frac{dV}{d(lnI)} \tag{3}$$

I_0 can be determined by an extrapolation of the forward bias ln(I)-V curve to V = 0 for each temperature. The zero bias barrier height (ϕ_b) is calculated by the following formula:

$$\phi_b = \frac{kT}{q}\ln\left(\frac{AA^*T^2}{I_o}\right) \tag{4}$$

The expression for the interface state density as deduced by Card and Rhoderick [21] is reduced to

$$N_{SS} = \frac{1}{q}\left[\frac{\varepsilon_i}{\delta}(n-1) - \frac{\varepsilon_s}{W_D}\right] \tag{5}$$

where d is the thickness of interfacial insulator layer, W_D is the width of the space charge region, ε_i and ε_s are the permittivity of the interfacial insulator layer and the semiconductor, respectively.

In Fig. 6, the semi-logarithmic I-V graph of n-Si/Ag Schottky diodes was produced at 200 K and 300 K substrate temperatures. The ln (I) -V curve of the n-Si/Ag Schottky diode produced at substrate temperature of 300 K shows a linear behavior between bias voltages of 0.2-1.5 V, while the diode produced at substrate temperature of 200 K shows a linear variation in the range of bias voltages of 0-0.7 V [18].

In Table 1, ideality factor (n) and saturation current (I_0) values of n-Si/Ag Schottky diodes produced at 200 K and 300 K substrate temperatures were calculated from ln (I)-V graph. As can be seen from the Table 1, Schottky diode at 300 K substrate temperature has higher n and I_0 values than 200 K substrate temperature production. However, the barrier height (φ_B) of the diode at a substrate temperature of 300 K is lower than that produced at 200 K. As is known, at a substrate temperature of 300 K, the Si surface Ag layer is coated with islets of different sizes. Thus, non-homogeneous regions were formed at the interface of the Si/Ag Schottky barrier [22-25]. This leads to a reduction in the barrier potential at the metal-semiconductor interface [26, 27].

The ideality factors of the samples are greater than 1, indicating that there are different current conduction mechanisms in the diodes.

The thermionic emission current-voltage relation of a Schottky diode with series resistance is given by [20]

$$I = I_0[e^{(q(V-IR_s)/nkT)} - 1] \tag{6}$$

Table 1. Experimental values of N_D, V_{FB}, N_{SS}, R_s, n, φ_B, I_0, and E_{00}.

Substrate Temperature	N_D (cm^{-3})	V_{FB} (V)	Nss (cm^{-3})	Rs (KΩ)	n	φ_B (eV)	I_0 (μA)	E_{00} (meV)
200 K	1.1×10^{15}	0.52	2.39×10^{12}	3.45	1.11	0.85	0.0014	0.49
300 K	1.4×10^{16}	0.34	2.72×10^{13}	5.51	3.68	0.78	0.05	1.60

where R_s is serial resistance. Eq. (6) can be differentiated as follows:

$$\frac{dV}{dln(I)} = \frac{nkT}{q} + IR_s \tag{7}$$

The series resistances are evaluated by using the slopes of dV/dln(I) versus I curves. Fig. 7 shows dV/dln(I) versus I plots for the n-Si/Ag (at 200 K and 300 K) Schottky diode.

From the experimental results, series resistance values of diodes were found. In Table 1, series resistance values are calculated from dV/dln (I) graph and are given. It is seen in the Table 1 that the diode prepared at 300 K substrate temperature has higher series resistance values than the diode prepared at 200 K substrate temperature. Increases in series resistance values are due to increases in surface state density in the metal-semiconductor interface area [28, 29].

Double Logarithmic I-V graph (Fig. 8) was used to determine the conduction mechanisms of the produced Si/Ag Schottky diodes. In Fig 8, Schottky diode produced at 300 K substrate temperature, 3 separate linear regions, two separate linear regions produced at 200 K substrate temperature were seen. Since the first region slope (m) of both diodes is greater than 2, the space charge limited current mechanism (SCLC) is effective in this region. In the second region, m <2 and omics behavior is exhibited. This shows that the tunneling current mechanism is dominant in the second region. In the third region of the Schottky diode produced at a substrate temperature of 300 K, m > 2, the Space Charge Limited Current mechanism (SCLC) is effective in this region.

In practice, tunneling mechanism is very significant for semiconductors that have E_{00} =10 value or a doping level higher than ~1×10^{17} cm^{-3} [10]. The carrier density of Schottky diode at substrate temperature of 300 K was found to be 1.1×10^{17} cm^{-3}. Therefore, the tunneling mechanism was investigated for n-Si/Ag structure. Tunneling mechanism can occur as two mechanisms: (1) field emission (FE) and (2) thermionic field emission (TFE). TFE theory is the dominant mechanism in the intermediate temperature and doping concentration, but FE theory is dominant only at quite low temperatures for the material having high doping concentrations [23]. Current-voltage relation for tunneling mechanism is given by [30,31]

$$I_t = I_{t0}(e^{(qV_d/E_0)}) \tag{8}$$

Where

$$E_0 = E_{00} coth\left(\frac{E_{00}}{kT}\right) \tag{9}$$

E_{00} is the characteristic energy; it is expressed as

$$E_{00} = \frac{h}{4\pi}\sqrt{\frac{N_d}{m_e^* \varepsilon_s}} \tag{10}$$

According to the theory, if $E_{00} >> kT$ is FE dominant, $E_{00} \sim KT$ is TFE dominant, and $E_{00} << kT$ is thermionic emission diffusion mechanism is dominant. In the Si/Ag Schottky diode produced at 200 K substrate temperature according to E_{00} values given in Table 1, it is found that the field thermionic emission diffusion mechanism is dominant. The field emission mechanism is dominant in the Si-Ag Schottky diode produced at a substrate temperature of 300 K.

Fig. 9 shows the Mott-Schottky graph measured at 1000 Hz frequency for Schottky diodes produced at 200 K and 300 K substrate temperatures. Typical results of C/V measurements for both types of diodes are displayed in Fig. 9. The constant slopes of the $1/C^2$ versus V curves indicate uniform doping profiles of the substrates and abrupt interfaces. Ideally, the capacitance (C) of a Schottky barrier is expressed from

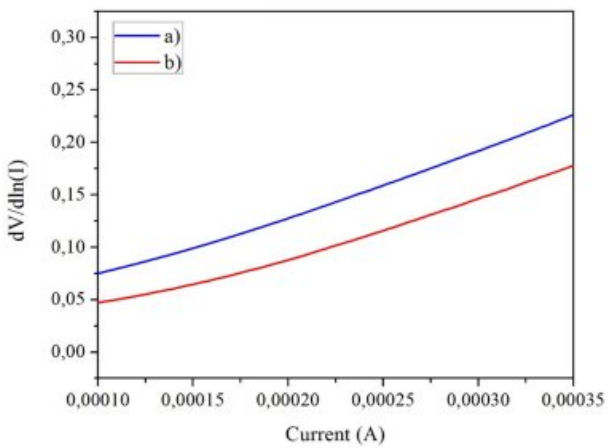

Fig. 7. Experimental dV/dln(I) versus I plots for the n-Si/Ag Schottky diode at (a) 200 K and (b) 300 K.

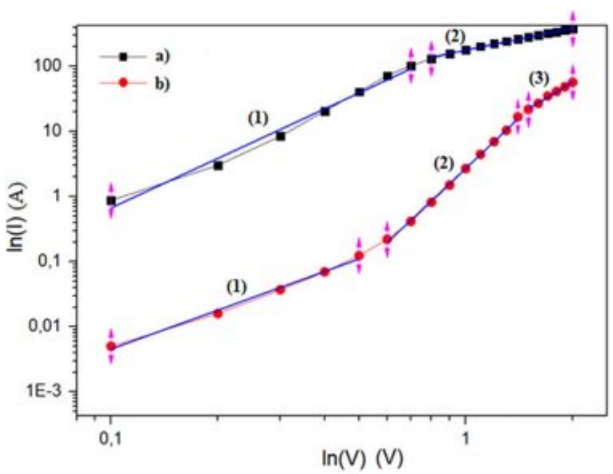

Fig. 8. Double logarithmic forward bias I-V plots of a n-Si/Ag Schottky diode at (a) 200 K and (b) 300 K.

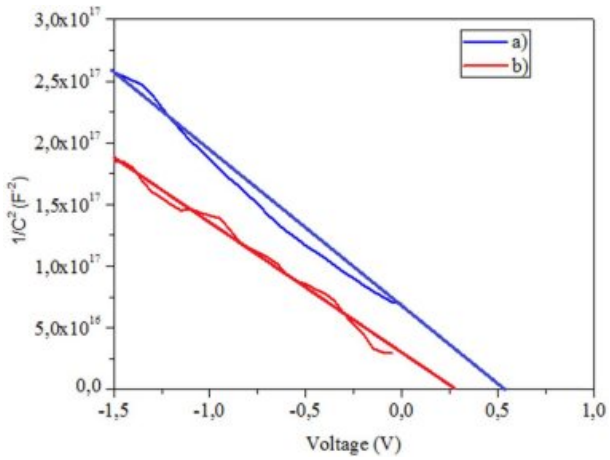

Fig. 9. Mott-Schottky graph of Si/Ag Schottky diodes (a) 200 K and (b) 300 K.

Eq. (11) [32, 33].

$$C^{-2} = \frac{2[V_d + V]}{q\varepsilon_0\varepsilon_s N_d S} \quad (11)$$

Where V is the applied potential, S is the active device area, N_d is the donor concentration, V_d is the diffusion potential, ε_0 is the vacuum dielectric constant and the relative dielectric constant εs. Where the curve in the graph is $1/C^2 = 0$ gives us the flat band potential (V_{FB}). Table 1 shows the V_{FB} values of Schottky diodes produced at 200 K and 300 K substrate temperatures. Donor densities in Si/Ag Schottky diodes were determined from linear regions of Mott Schottky curves.

Table 1 shows N_D, V_{FB} and N_{SS} values calculated from C-V measurements. The donor density was found to be lower at the 200 K substrate temperature than the 300 K substrate temperature. The surface state density (N_{SS}) at the metal-semiconductor interface was calculated to be lower in the Schottky diode produced at a substrate temperature of 200 K compared to a substrate temperature of 300 K.

Conclusion

In this study, Schottky diodes were produced by evaporating Ag onto n-Si using vacuum evaporation technique at 200 K (cold substrate) and 300 K substrate temperature. It was seen from the FESEM images that the Ag layer was composed of equal sized nano clusters at 200 K substrate temperature and that the Ag layer was composed of islets of different size at 300 K substrate temperature. When the photocurrent values were examined according to wavelength, SPR effect was observed in Ag thin film produced at 200K substrate temperature at 470 nm wavelength (638 THz). Si/Ag Schottky diode produced at 200 K substrate temperature from I-V measurements had better rectification properties. In the experiments, n, I_0 and Rs values of Schottky diode produced at 300K substrate temperature were higher than those produced at 200 K substrate temperature. It was understood from the obtained results that transmission at 200 K and 300 K substrate temperatures can be controlled by tunneling at low bias voltages and SCLC at high bias voltages.

References

1. S.M. Sze, in "Semiconductor Devices: Physics and Technology", (John Wiley & Sons, 2008) p. 84.
2. B. Sahin, H. Cetin, and H. Ayyildiz, Solid State Commun. 135 (2005) 490-495.
3. S. Karatas, Microelectron. Eng. 87 (2010) 1935-1940.
4. M.E. Aydin, K. Akkilic, and T. Kilicoglu, Physica B. 352 (2004) 312-317.
5. Z. Ahmad and M.H. Sayyad, Physica E. 41 (2009) 631-634.
6. S. Guduru, V.P. Singh, S. Rajaputra, S. Mishra, R. Mangu, and St. Omer, Thin Solid Films 518 (2010) 1809-1814.
7. V. Nevruzoglu, M. Tomakin, E.F. Keskenler, and G. Ozturk, J. Ceram. Process. Res.18 (2017) 494-500.
8. F.K. Konana, A. Betiéd, H.J.T. Nkuissib, K. Dakshib, B. Akaa, and B. Hartitib, J. Ceram. Process. Res. 18 (2017) 882-886.
9. M. Amuthasurabi, J. Chandradass, V.R. Babu, P.B. Sethupathi, and M.L.J. Martin, J. Ceram. Process. Res. 18 (2017) 815-818.
10. E. Bingöl, F. Bozali, E.F. Keskenler, V. Nevruzoğlu, and M. Tomakin, Turk. J. Mater 1 (2016) 19-24.
11. M. Okutan and F. Yakuphanoğlu, Microelectron. Eng. 85 (2008) 646-653.
12. C.W. Bates, J.C. White, and C. Ekeocha, 143 (2007) 38-41.
13. O.H. Mahmood, A.G. İmer, and A. Korkut, ICSMD-2018, 1 (2019) 47-51.
14. D. Korosak and B. Cvikl, ASDAM '98, 1 (1998) 137-140.
15. W. Clayton, J. Bates, and C. Zhang, Aip Advances 3 (2013) 1-15.
16. G.D. Yüzüak, E. Yüzüak, V. Nevruzoğlu, and İ. Dinçer, Applied Physics A. 125 (2019) 794-803.
17. F. Heıdarpour, W.A. Wan, AB Karım Ghanı, F.R. Bın Ahmadun, S. Sobrı, M. Zargar, and M.R. Mozafarıa, Dig. J. Nanomater. Bios. 5 (2010) 787-796.
18. M. Tomakin, M. Altunbaş and E. Bacaksız, Physica B. 406 (2011) 4355-4360.
19. K.C. Lee, S.J. Lin, C.H. Lin, C.S. Tsai, and Y.J. Lu, Surf. Coat. Technol. 202 (2008) 5339-5342.
20. D.K. Schroder, in "Semiconductor Materials and Device Characterization", (Wiley, New York, 1990) p. 190.
21. H.C. Card and E.H. Rhoderick, J. Phys. D: Appl. Phys. 4 (1971) 1589-1601.
22. R.T. Tung, Mater. Sci. Eng. R: Rep. 35 (2001) 1-138.
23. S. Oktik, G.J. Russell, and J. Woods, Semicond. Sci. Technol. 2l (1987) 661-665.
24. K. Patel, K.K. Nanda, and S.N. Sahu, J. Appl. Phys. 85 (1999) 3666-3670.
25. V.V. Kislyuk, M.I. Fedorchenko, P.S. Smertenko, O.P. Dimitriev, and A.A. Pud, J. Phys. D: Appl. Phys. 43 (2010) 185301-185311.
26. R.T. Tung, Phys. Rev. B 45 (1992) 13509-13523.
27. J.H. Werner and H.H. Guttler, J. Appl. Phys. 69 (1991) 1522-1533.
28. A. Keffous, M. Siad, S. Mamma, Y. Belkacem, C.L.

Chaouch, H. Menari, A. Dahmani, and W. Chergui, Appl. Surf. Sci. 218 (2003) 336-342.
29. J.H. Lee, J.S. Yi, K.J. Yang, J.H. Park, and R.D. Oh, Thin Solid Films 431 (2003) 344-348.
30. F.A. Padovani and R. Stratton, Solid-State Electron 9 (1966) 695-707.
31. C.R. Crowell and V. L. Rideout, Solid-State Electron 12 (1969) 89-105.
32. S.M. Sze, in "Physics of Semiconductor Devices" (Wiley Eastern Limited, 3rd edition, 1985) p. 170.
33. E.H. Rhoderic and R.H. Williams, in "Metals Semiconductor Contacts" (Oxford University Press, 1988) p. 48.